Published in final edited form as:

Nat Microbiol. 2018 May ; 3(5): 556–562. doi:10.1038/s41564-018-0141-7.

A cynomolgus macaque model for Crimean-Congo haemorrhagic fever

Elaine Haddock[1], **Friederike Feldmann**[2], **David W. Hawman**[1], **Marko Zivcec**[1,3,5], **Patrick W. Hanley**[2], **Greg Saturday**[2], **Dana P. Scott**[2], **Tina Thomas**[2], **Miša Korva**[4], **Tatjana Avšič-Županc**[4], **David Safronetz**[1,6], **Heinz Feldmann**[1,*]

[1]Laboratory of Virology, Division of Intramural Research, National Institute of Allergy and Infectious Diseases, National Institutes of Health, Hamilton, MT, USA.

[2]Rocky Mountain Veterinary Branch, Division of Intramural Research, National Institute of Allergy and Infectious Diseases, National Institutes of Health, Hamilton, MT, USA.

[3]Department of Medical Microbiology, University of Manitoba, Winnipeg, Manitoba, Canada.

[4]Laboratory for Diagnostics of Zoonoses and WHO Centre, Institute of Microbiology and Immunology, Faculty of Medicine, University of Ljubljana, Ljubljana, Slovenia.

[5]Viral Special Pathogens Branch, Centers for Disease Control and Prevention, Atlanta, GA, USA.

[6]Special Pathogens Program, National Microbiology Laboratory, Public Health Agency of Canada, Winnipeg, Manitoba, Canada.

Abstract

Crimean-Congo haemorrhagic fever (CCHF) is the most medically significant tick-borne disease, being widespread in the Middle East, Asia, Africa and parts of Europe[1]. Increasing case numbers, westerly movement and broadly ranging case fatality rates substantiate the concern of CCHF as a public health threat. Ixodid ticks of the genus *Hyalomma* are the vector for CCHF virus (CCHFV), an arbovirus in the genus *Orthonairovirus* of the family Nairoviridae. CCHFV naturally infects numerous wild and domestic animals via tick bite without causing obvious disease[2,3]. Severe disease occurs only in humans and transmission usually happens through tick bite or contact with infected animals or humans. The only CCHF disease model is a subset of immunocompromised mice[4–6]. Here, we show that following CCHFV infection, cynomolgus macaques exhibited

[*]**Correspondence and requests for materials** should be addressed to H.F. feldmannh@niaid.nih.gov.

Author contributions

E.H. and H.F. planned the study. E.H., F.F., M.Z., P.W.H., G.S, D.P.S. and D.S. conducted the non-human primate work. E.H., F.F., D.W.H., P.W.H., G.S., D.P.S. and T.T. acquired the data. E.H., P.W.H., G.S., D.H., M.K., T.A.-Z. and H.F. analysed and interpreted the data. M.K. and T.A.-Z. provided critical reagents. E.H. and H.F. wrote the first draft. All authors reviewed, edited and approved the paper.

Competing interests

The authors declare no competing interests.

Supplementary information is available for this paper at https://doi.org/10.1038/s41564-018-0141-7.

Data availability. The data supporting the findings of this study are available within the paper and its supplementary information files, or from the corresponding author upon request.

hallmark signs of human CCHF with remarkably similar viral dissemination, organ pathology and disease progression. Histopathology showed infection of hepatocytes, endothelial cells and monocytes and fatal outcome seemed associated with endothelial dysfunction manifesting in a clinical shock syndrome with coagulopathy. This non-human primate model will be an invaluable asset for CCHFV countermeasures development.

Life Sciences Reporting Summary.

Further information on experimental design is available in the Life Sciences Reporting Summary.

Human CCHF disease shows a wide range of severity, from a mild, non-specific febrile illness to shock and death. It is characterized by four distinct phases. Incubation generally lasts 1–7 days following exposure[2]. The prehaemorrhagic phase lasts 3–7 days and is distinguished by a sudden onset of symptoms including headache, malaise and fever, and may also yield diarrhoea, nausea and vomiting[4]. Severe cases may develop haemorrhaging including petechiae and/or ecchymoses, gingival bleeds and epistaxis, and can progress to multiorgan failure[7–9]. Survivors face a long convalescence that may include such symptoms as vision, hearing and memory loss, tachycardia, and breathing impairment[1,10]. Clinical laboratory parameters include thrombocytopenia, leukopenia, coagulopathy and elevated liver enzymes[10]. The case fatality rate is approximately 30% overall[10,11], but varies geographically, from 5% in Turkey[12] to 60% in the United Arab Emirates[9,13,14]. Currently, no approved vaccine against CCHFV is available. The only effective means of preventing CCHFV infection are avoiding tick bites, safe slaughtering of livestock and universal healthcare precautions[10]. Ribavirin, recommended by the World Health Organization to treat CCHF patients, has unclear efficacy[15,16].

Previous CCHFV infection studies in non-human primates (NHPs) have resulted in a lack of both clinical signs and fulminant disease[17,18]. Other experimentally infected animals, including livestock, guinea pigs, rabbits and hamsters, yield varying degrees of viraemia and high levels of neutralizing antibody but no clinical disease[3]. In recent years, mice deficient in the type I and II interferon system have been revealed as useful animal models for severe CCHFV[4–6]. Unfortunately, despite the similarities to human CCHF disease, countermeasure research is hindered by the lack of an immunocompetent, higher mammal model for licensing requirements.

Here, we introduce a disease model by infection of cynomolgus macaques with CCHFV Kosova Hoti (hereafter CCHFV Hoti)[19]. Initial studies in rhesus macaques infected with either CCHFV IbAr 10200 or CCHFV Hoti via several routes of inoculation resulted in no overt disease. Similar lack of disease was seen in African green monkeys with CCHFV Hoti. However, in a pilot study of infection with 1×10^5 $TCID_{50}$ (tissue culture infectious dose, 50%) CCHFV Hoti in cynomolgus macaques ($n = 3$), one subcutaneous- and the single subcutaneous/intravenous (SC/IV)-inoculated animal developed disease including thrombocytopenia, hypoproteinemia, oedema and epistaxis; both animals were euthanized according to IACUC (Institutional Animal Care and Use Committee)-approved endpoint criteria including oedema and frank bleeding (Supplementary Fig. 1)[20].

Based on our pilot studies, we infected 12 cynomolgus macaques with CCHFV Hoti (1×10^5 $TCID_{50}$) by either the subcutaneous or intravenous route, or by the combined SC/IV route ($n = 4$). Daily scoring revealed signs of disease by 3 days post-infection (dpi) in the SC/IV group, with the intravenous group scores lagging (Fig. 1a). Only two subcutaneous-infected animals developed mild clinical signs. In intravenous- and SC/IV-infected animals, early clinical signs included piloerection, anorexia and hunched posture. Elevated temperature was noted at 1 dpi in some animals (1 of 4 SC/IV, 2 of 4 intravenous, 0 of 4 subcutaneous) with no significant difference among groups. Furthermore, clinical signs in all eight SC/IV- and intravenous-infected animals also involved lethargy and facial and body oedema (including scrotal oedema in males), evident as early as 4 dpi. In some cases, facial oedema began to abate in later disease stages (6–7 dpi), leaving behind periocular bruising. Additionally, at 6–7 dpi epistaxis (5 of 8), haematochezia (2 of 8), gingival haemorrhage, petechiae of ventral thorax, arms, and face (4 of 8) and an increased bleeding tendency, including deep tissue haemorrhaging reminiscent of human ecchymosis, were observed. There was no apparent difference in disease manifestations between male and female macaques. Disease severity peaked at 7 dpi and survival was assessed at 100% (2 mild, 2 asymptomatic) in the subcutaneous-, 25% (3 fatal, 1 severe) in the intravenous- and 75% (1 fatal, 3 severe) in the combined SC/IV-infected group (Fig. 1b) following IACUC-approved humane endpoint criteria[20]. All animals that survived to 9 dpi entered convalescence.

Viraemia, as measured by viral RNA in whole blood and presented as infectivity equivalents, peaked in SC/IV- and intravenous-infected animals at 3 dpi (Fig. 1c), coinciding with the onset of clinical signs, and then declined as clinical signs increased in severity. Animals infected subcutaneously developed peak viraemia later (5 dpi) followed by a decrease over the following days. Virus isolation of 3 dpi blood samples (1:100 and/or 1:1,000 dilution) yielded infectious virus from all SC/IV- or intravenous- and from a single subcutaneous-infected animal. Low levels of viral RNA were detectable in swabs (oral, nasal and rectal) and urine between 3 dpi and 9 dpi, particularly in animals infected by the intravenous or SC/IV routes (Supplementary Fig. 2), but virus could not be isolated.

All SC/IV and two of four animals in the intravenous group were leukopenic, equally neutropenic and lymphopenic, at 5 dpi in contrast to the subcutaneous group. All of the SC/IV and three of four of the intravenous animals developed thrombocytopenia with marked reduction in platelet levels by 5 dpi (Fig. 1d). SC/IV- and intravenous-infected animals developed hypoproteinemia (Fig. 1e) and hypoalbuminemia (Fig. 1f). Aspartate aminotransferase and alanine aminotransferase were elevated (Fig. 1g,h), indicating hepatocellular liver disease starting at 3 dpi in all of the SC/IV- and intravenous- but only two subcutaneous-infected animals. Clotting of several animals was compromised, as determined by calculated coagulation times (Fig. 1i,j). Activated partial prothrombin times and thrombin times were extended as early as 3 dpi in SC/IV-infected animals and peaked during the haemorrhagic phase. Normalization of platelets, total protein, liver enzymes and clotting times at 9 dpi were indicative of the onset of convalescence.

Serum levels of both interleukin-6 (IL-6) and IL-10 were elevated in all three groups of NHPs by 3 dpi, as clinical signs become apparent (Fig. 2a,b). While IL-6 levels dropped substantially in all groups by 7 dpi, IL-10 levels remained high into convalescence. When

focusing on disease severity rather than infection route (Supplementary Fig. 3a,b), the asymptomatic animals in the sub-cutaneous group had no IL-6 or IL-10 response, and the early IL-6 response between fatal and severe but surviving cases was distinct. Increased levels of inflammatory marker IL-1RA by 3 dpi (Fig. 2d, Supplementary Fig. 3d) indicated a strong inflammatory response to CCHFV infection, as did the increases in inflammatory chemokines MCP-1 and MIP-1β (Fig. 2e,f, Supplementary Fig. 3e,f). IL-1β levels rose slightly at 3 dpi and continued to rise through disease into convalescence (Fig. 2c, Supplementary Fig. 3c) as IL-1RA and chemokine levels fell. IL-15 (Fig. 2g, Supplementary Fig. 3g), a mediator of cell proliferation, closely followed the time course of MCP-1. IL-17A, a proinflammatory cytokine released by activated T cells, was elevated later in infection (Fig. 2h, Supplementary Fig. 3h), with the strongest response coming from severely ill but surviving animals and from animals that were asymptomatic. All animals displayed significant IgM and IgG production against CCHFV by 7 dpi (Supplementary Fig. 4a,b), confirming CCHFV exposure by all routes. Neutralizing activity was low as expected for the early time points and does not appear to correlate with disease outcome (Supplementary Fig. 5).

Animals were euthanized either based upon IACUC-approved humane endpoint[20] (4 total: 1 SC/IV, 3 intravenous; 6 or 7 dpi), at onset of convalescence (1 SC/IV, 1 intravenous; 8 or 9 dpi) or (2 SC/IV, 4 subcutaneous) for comparative pathology at 12 dpi. Both animals euthanized at the onset of convalescent were recovering from severe illness and euthanasia was allowed for comparisons between fatality, convalescence, recovery and absence of disease. Within the subcutaneous group, one animal presented with haematochezia, enlarged inguinal lymph nodes and pale kidneys at 12 dpi. Of the three terminal animals in the intravenous-infected group, a male presented with facial oedema and severe abdominal distension (6 dpi). One female was noted to have a combination of frank bleeding, ataxia, petechia and a lack of urine/faecal output and food intake; the second female was scored for frank bleeding and oedema (both 7 dpi). The intravenous-infected animals uniformly exhibited pale livers with hepatomegaly and enlarged mediastinal lymph nodes; additionally, two animals had epistaxis, one animal had facial oedema, ileus with clear peritoneal fluid and lungs that failed to collapse, and one animal had caecal and colonic serosal haemorrhage. The single terminal animal within the SC/IV-infected group presented with facial, scrotal and body oedema with laboured breathing, petechia and a reluctance to move (7 dpi). Animals within this SC/IV inoculation group displayed pale livers with hepatomegaly in three of four animals, epistaxis in two animals, splenomegaly in two animals and one animal had subcutaneous oedema and oedematous lungs that failed to collapse.

The highest tissue viral RNA yields were from lymph nodes (cervical, axillary, inguinal and bronchial), liver, spleen, adrenal gland and kidney (Supplementary Fig. 6), mirroring the histopathology results (Fig. 3, Supplementary Fig. 7). Overall, viral RNA recovery from subcutaneous-infected animals was lower than from intravenous- or SC/IV-infected animals, as expected due to both reduced disease severity and to the 12 dpi euthanasia date of this group, but RNA was still detectable in each tissue in at least two animals. Additionally, viral RNA was also detectable in bone marrow (2 subcutaneous, 4 intravenous, 4 SC/IV), bladder (2 subcutaneous, 3 intravenous, 3 SC/IV), male and female reproductive organs (2

subcutaneous, 4 intravenous, 3 SC/IV) and brain (2 subcutaneous, 4 intravenous, 4 SC/IV). While some tissues did yield live virus (Supplementary Fig. 6, denoted by *, 1:100 and/or 1:1,000 dilution), virus isolation was inconsistent as to infection route, disease severity and time of euthanasia and much less sensitive than RNA quantitation.

Histopathology was most prominent in the liver. Moderate lym-phohistiocytic hepatitis was identified via the combined infection route while minimal hepatitis was identified in the subcutaneous route. The principle finding was mild-moderate lymphohistiocytic infiltrate with multifocal hepatic necrosis, fibrin thrombi and moderate vacuolar change (Fig. 3a–c). Both immunohistochemistry (Fig. 3d–f) and in situ hybridization (Fig. 3g–i) revealed infection of hepatocytes, Kupffer and endothelial cells. Overall, the spleen showed moderate congestion with random fibrin thrombi in the red pulp with lymphocytolysis of the white pulp in one animal (Supplementary Fig. 7a–c). Viral antigen detection by immunohistochemistry in the spleen was minimal at necropsy (Supplementary Fig. 7d–f), but viral RNA was detected at varying levels in the splenic pulp (Supplementary Fig. 7g–i). In situ hybridization detected positive-sense RNA in multiple tissues indicating replication with the same pattern of highest yield from the combined infection route, followed by intravenous alone, and little replication visible in sub-cutaneous-infected animals (Supplementary Fig. 8). Positive-sense RNA was detected in hepatocytes, Kupffer and endothelial cells of the liver and marginal zone lymphocytes of the spleen and lymphnodes. Immunoreactivity was noted in endothelial and interstitial cells of the kidney and in cortical, medullary and endothelial cells of the adrenal gland.

Most previous research pertaining to CCHF has been conducted using reference strain CCHFV IbAr 10200, isolated from a tick in Nigeria followed by sequential passage in suckling mice and tissue culture[21]. Our pilot study in rhesus macaques utilizing IbAr 10200 confirmed previous unsuccessful attempts to cause disease (Supplementary Fig. 1). CCHFV Hoti, which was isolated from blood of a fatal human case, originated from an endemic region in Kosova with high case fatality rates[19]. Phylogenetically it clusters with Russian CCHFV strains and is quite distinct from IbAr 10200[22]. CCHFV Hoti infection of different NHP species resulted in a range of outcomes (Fig. 1, Supplementary Fig. 1). Therefore, outcome of infection could be associated with the origin of the isolate (vector versus host), the adaptation status of the strain (passage history) and the NHP species, as has been discussed for hantaviruses[23]. These distinct outcomes provide an opportunity for future studies investigating the host factors that control CCHFV infection.

IV inoculation was important for causing more severe disease in cynomolgus macaques. Overall, the course of disease appears as a 3–4 day preincubation period, followed by approximately 3–5 days of a prehaemorrhagic phase which, in some animals, was followed by a haemorrhagic phase of 2–3 days, with convalescence beginning at approximately 9 dpi (Fig. 4). This is remarkably like what has been described for human CCHF[2,11,13]. The varying outcome of CCHFV Hoti infection in cynomolgus macaques now allows for studying host and viral factors involved in pathogenesis and disease outcome.

The overarching pattern of early viraemia and inflammatory response, followed by thrombocytopenia, coagulation disorder, elevated liver enzyme and metabolic imbalances

(Figs. 1 and 4) correlates with human CCHF progression. CCHFV replicated in macaque hepatocytes, Kupffer and endothelial cells of the liver, as previously reported in humans[24], and marginal zone lymphocytes of the spleen and lymph nodes. Immunoreactivity confirmed viral replication through the lymphatic system and notable major organs at the time of euthanasia. The involvement of endothelial cells, taken with the elongated coagulation times (Fig. 1i,j), suggest inflammatory damage through the intrinsic coagulation pathway. In animals that succumbed to disease, the most likely cause of death was endothelial dysfunction manifesting in a clinical shock syndrome with coagulation abnormalities.

The role of proinflammatory cytokines for the pathogenesis of human CCHF has been discussed[25–28]. Increased cytokine expression may contribute to capillary leakage and oedema formation as discovered here in CCHFV Hoti-infected macaques (Fig. 4). Symptomatic animals displayed a strong systemic early inflammatory response (Fig. 2, Supplementary Fig. 3) and increases in IL-17A during peak disease into convalescence may be an attempt to moderate this inflammatory response. As with humans[26–29], chemokines play a role in NHP disease (Fig. 2, Supplementary Fig. 3). In contrast to humans, elevated levels of TNFa were not detected in infected macaques.

In summary, the cynomolgus macaque model remarkably recapitulates the hallmark clinical and pathological framework of human CCHF in an immunocompetent animal (Fig. 4). A uniformly lethal model would be ideal for CCHFV countermeasure development; however, this may not be possible. Such efforts may have to include passaging of CCHFV into naive macaques, something to consider for future work. Nevertheless, the current macaque model is invaluable for pathogenesis and immunologic studies as the model induces similar wide-range responses to those seen in humans. Responses ranging from asymptomatic disease to fatality, with and without haemorrhage, allow the macaque model to be utilized to study disease mechanisms induced by CCHFV infection. As the only immunocompetent CCHF animal model currently, it will also be instrumental in the evaluation of countermeasures against CCHFV.

Methods

Biosafety and animal ethics.

All infectious work with CCHFV and sample inactivation was performed in the maximum containment laboratory in accordance with standard operating procedures approved by the Rocky Mountain Laboratories Institutional Biosafety Committee, Division of Intramural Research, National Institute of Allergy and Infectious Diseases, National Institutes of Health (Hamilton, MT, USA). All animal work was performed in strict accordance with the recommendations described in the Guide for the Care and Use of Laboratory Animals of the National Institutes of Health, the Office of Animal Welfare and the US Department of Agriculture in an Association for Assessment and Accreditation of Laboratory Animal Care International (AAALAC)-accredited facility. Animals were housed in adjoining individual primate cages that enabled social interaction, under controlled conditions of humidity, temperature and light (12-h light/12-h dark cycles). Food and water were available ad libitum. Animals were monitored at least twice daily (pre- and post-infection) and fed commercial monkey chow, treats and fruit twice a day by trained personnel. Environmental

enrichment consisted of manipulanda, visual enrichment and audio enrichment. Humane endpoint, specified and approved by the IACUC, was applied to determine when animals should be humanely euthanized[20]. Clinical score criteria may be shared upon request.

CCHFV stocks.

IbAr 10200 was kindly provided by Dr Michael Holbrook (at the time University of Texas Medical Branch, Galveston), confirmed as negative for *Mycoplasma spp.* and passaged once to grow a stock. The entire prior passage history is largely unknown, but included passaging through suckling mouse brains and tissue culture cells. CCHFV Hoti (p7, provided through the European Virus Archive, https://www.european-virus-archive.com/), a low passage virus never passaged through mice, was propagated with treatment to remove *Mycoplasma spp.* and passaged once with additional treatment to confirm as negative for *Mycoplasma spp.* before passaging once more to grow a p9 stock. Both viruses were propagated in SW13 (ATCC CCL-105; not authenticated but proven mycoplasma-free in our laboratory) with 2% FBS, L-glutamine (40 μM) and penicillin/ streptomycin (500 units per ml and 500 μg per ml), then harvested, spun for clarification, aliquoted and frozen in liquid nitrogen with 20% FBS and 100 mM HEPES buffer. Viral stocks were diluted to challenge dose in DMEM (Sigma-Aldrich).

Deep sequencing of our CCHFV Hoti stock was performed and the sequences aligned to the available sequences on Genbank (accession numbers EU044832.1, EU037902.1, DQ133507.1). Sequencing revealed four mutations present in the M segment of our CCHFV Hoti stock. The first two mutations (nt 346 A >T D90V) and (nt 763 T > C, L229P) were in the mucin-like protein. The third (nt 2992 C > A A972D) and fourth (nt 2799 G > A, G908S) were in the NSm protein of the M segment. These mutations were present in 11%, 40%, 35% and 8% of reads, respectively. Two mutations were also found in the L segment: nt 5919 A > T N1948Y and nt 11238 A > G, T3721A. They were present in 3% and 37% of reads, respectively.

Pilot studies.

Four rhesus macaques (*Macaca mulatto*) (2 male and 2 female, age 4 years, weight range 4–6 kg) were challenged with 2×10^6 TCID50 IbAr 10200 by intratracheal, intravenous and subcutaneous inoculation (four sites on the cranial dorsum). Four rhesus macaques (2 male and 2 female, age 3 years, weight range 3–5 kg) were challenged with 1×10^5 $TCID_{50}$ CCHFV Hoti by intravenous and subcutaneous inoculation. Four African green monkeys (*Chlorocebus sabaeus*) (2 male and 2 female, age 1–5 years, weight range 3–6 kg) were challenged with 1×10^5 TCID50 CCHFV Hoti by intravenous and subcutaneous inoculation (four sites on the cranial dorsum). Cynomologus macaques (*Macaca fascicularis*) were challenged either subcutaneously (1 male and 1 female, age range 5–7 years, weight range 3–6 kg) or SC/IV (1 male, 6 years, 8 kg). The challenge dose was confirmed by back-titration of the inoculum on SW13 cells. A physical examination including collection of blood and mucosal swabs was conducted at predetermined examination days (0, 1, 3, 5, 7, 9 and 12) and at terminal endpoints. Animal numbers were not based on power analysis but rather on experience with similar studies, group assignment was randomized as best as possible and only personnel for clinical scoring and pathology were blinded.

Study design.

Twelve cynomolgus macaques (*Macaca fascicularis*) (6 male and 6 female, age range 3–5 years, weight range 3–6 kg) were used in this study at 4 animals per group (1 older/1 younger male, 1 older/1 younger female; animal numbers per group were based on experience with similar studies rather than meaningful power analysis). Groups were challenged with 1×10^5 $TCID_{50}$ CCHFV Hoti by one of three methods: subcutaneously divided in four sites on the cranial dorsum, intravenously through the saphenous vein, or a combination of SC/IV using half the dose subcutaneously and half intravenously. The challenge dose was confirmed by back-titration of the inoculum on SW13 cells. A physical examination including collection of blood and mucosal swabs was conducted at predetermined examination days (0, 1, 3, 5, 7, 9 and 12) and at terminal endpoints. Full necropsies were performed on each animal and organs were harvested for virologic and pathologic analyses. Only personnel for clinical scoring and pathology were blinded.

Haematology, serum biochemistry and coagulation analyses.

Haematology was completed on a Procyte DX (IDEXX Laboratories) and the following parameters were evaluated: red blood cells, haemoglobin, haematocrit, mean corpuscular volume, mean corpuscular haemoglobin, mean corpuscular haemoglobin concentration, red cell distribution weight, platelets, mean platelet volume, white blood cells, neutrophil count (absolute (abs) and %), lymphocyte count (abs and %), monocyte count (abs and %), eosinophil count (abs and %) and basophil count (abs and %). Serum chemistries were completed on a Piccolo Xpress (Abaxis) and the following parameters were evaluated: glucose, blood urea nitrogen, creatinine, calcium, albumin, total protein, alanine aminotransferase, aspartate aminotransferase, alkaline phosphatase, total bilirubin, gamma glutamyltransferase and amylase. Coagulation values were determined from citrated plasma utilizing the STart4 Hemostatis Analyzer (Diagnostica Stago) and associated testing kits also from Diagnostica Stago.

Histopathology.

Histopathology, immunohistochemistry and in situ hybridization were performed on macaque tissues. Following fixation and inactivation of tissues (< 1 cm^3) for a minimum of 7 days in 10% neutral-buffered formalin and one formalin exchange (Institutional Biosafety Committee-approved protocol), tissues were removed from BSL4 and processed using a VIP-6 Tissue Tek (Sakura Finetek) tissue processor and embedded in Ultraffin paraffin polymer (Cancer Diagnostics). Samples were sectioned at 5 pm and resulting slides were stained with haematoxylin and eosin. Anti-CCHF virus immunoreactivity was detected using a custom rabbit anti-NP antibody (peptide sequence KDEMNRWFEEFKKGNGLVD) (Open Biosystems) at 1:1,500 dilution. The secondary antibody was a ready-to-use biotinylated anti-rabbit antibody (predilute; Biogenex). The tissues were processed for immunohistochemical staining using the Discovery Ultra automated staining platform (Ventana Medical System) with a Discovery DABMap kit. Detection of CCHF viral RNA was performed using the RNAscope 2.5 VS assay (Advanced Cell Diagnostic Inc.) on the Ventana Discovery ULTRA as previously described[30] and in accordance with the manufacturer's instructions. Briefly, tissue sections were deparaffinized and pretreated with

heat and protease before hybridization with either sense or antisense probes specific to the glycoprotein precursor (GPC) region of the CCHFV genome. Peptidylprolyl isomerase B (Ppib) and the bacterial gene, *dapB*, were used as positive and negative controls, respectively.

CCHFV RNA detection.

Total RNA was extracted from blood, swabs and urine samples using QIAamp Viral RNA extraction kits or from tissue samples using RNeasy extraction kits (Qiagen) and tested for the presence of CCHFV RNA by quantitative real-time one-step RT-PCR using a Rotor-Gene RG-3000 instrument, QuantiFast Probe RT-PCR + ROX Vial Kit (Qiagen), primers specific to the CCHFV S segment (forward: 5' CTTTGCTCATGACTCTTTCCAG and reverse: 5' TCCGAAGGTTGAGAATGGAC, 0.4 μM final concentration) and a dual-labelled fluorescent probe (6FAM-TGTCCAGATCCCTGAGCAGCGTC, 0.2 p M final concentration) (all from TIB Molbiol). RT-PCR was carried out in three stages: reverse transcription (50°C for 30 min), Taq activation (95°C for 5 min) and amplification (40 cycles of 95°C for 15 s and 60°C for 15 s) of each amplification cycle. Samples were quantified against a standard curve of CCHFV Hoti RNA extracted from viral stock with predetermined titre and calculated as infectivity equivalents ($TCID_{50}$ per ml or $TCID_{50}$ per g).

Virus isolation.

Isolation was conducted on SW13 cells plated for 80% confluency in 48-well plates. Medium was removed from cells and replaced with 1:100 and/or 1:1,000 dilutions of blood, swab medium or urine in 0.1 ml, with an infection time of 45 min, following which the inoculum was removed, cells were washed once with Dulbecco's phosphate buffered saline (PBS) and 0.5 ml L-15 with 2% FBS, penicillin/streptomycin and L-glutamine was added. Tissues were weighed in 1 ml L-15 with a 5 mm stainless steel bead, homogenized at 30 Hz for 10 min, spun at 8,000 rpm for 10 min and diluted 1:100 or 1:1,000 and used to infect SW13 cells as above. All cells were read for cytopathic effect at day 4 for evidence of virus.

Antibody analyses.

CCHF-specific IgM and IgG were measured by enzyme-linked immunosorbent assay (ELISA). CCHF antigen for ELISA was prepared by infecting SW13 cells with CCHFV Hoti and collecting supernatant at 48 hours post-infection. The virus was then pelleted by ultracentrifugation through a 20% sucrose cushion. The viral pellet was resuspended in PBS + 2% Triton-X 100 and irradiated with 10 megarad (Mrad) of γ-radiation by a JL Shepherd Model 484 irradiator with cobalt cell. Mock antigen was prepared similarly from mock-infected SW13 cells. Amount of total protein in mock and CCHF antigen samples was quantified by detergent-compatible bicinchoninic acid assay (Thermo Fisher) against bovine serum albumin standards. Equivalent amounts of protein diluted in PBS were then adsorbed to Nunc Maxisorp plates. Plates were blocked with 5% skimmed milk in PBS + 0.05% Tween-20 and then washed with PBS + 0.05% Tween-20. Serial twofold dilutions of serum in blocking buffer (5% skimmed milk in PBS + 0.05% Tween-20) beginning with the 1:200 dilution were then applied to plates. Plates were washed extensively with PBS + 0.05% Tween-20 and bound antibody detected with peroxidase-labelled goat anti-monkey IgG

(SeraCare) or goat anti-monkey IgM (Fitzgerald). Plates were washed extensively and plates developed with 2, 2'-azino-di(3-ethylbenzthiazoline-6-sulfonate) and reaction terminated with 5% sodium dodecyl sulfate (Sigma) in water. Absorbance at 405 nm was measured. Endpoint titres were defined as the reciprocal of the last dilution to have an absorbance ≥0.2.

Neutralization assay.

Neutralizing activity in the serum was measured by focus reduction neutralization test. Serum was heat inactivated at 56°C for 30 min. Heat-inactivated serum was then serially twofold diluted in L-15 media supplemented with 2% heat-inactivated foetal bovine serum, penicillin and streptomycin beginning with the 1:20 dilution. Diluted serum was then challenged with approximately 50 focus-forming units of CCHFV Hoti, gently mixed and incubated at 37°C for 1 h. Remaining infectious virus was measured by focus-forming assay. For this, SW13 cells were plated in 96-well plates at 10,000 cells per well in 100 μl of L-15 media supplemented with 10% foetal bovine serum, penicillin and streptomycin. The next day, supernatant was removed, and 50 μl of sample applied to well and allowed to incubate for 2 h at 37°C. Sample was then removed and cells overlaid with L-15 media supplemented with 2% fetal bovine serum, penicillin, streptomycin and 0.8% methylcellulose (Sigma). Cells were incubated at 37°C for 40 h. Overlay was then removed, and cells washed once with PBS and fixed with 2% paraformaldehyde overnight at 4°C. Plates were then removed from the BSL4 according to approved procedures. Plates were washed three times with PBS and once with permwash (PBS + 0.05% saponin+ 0.1% bovine serum albumin). To detect CCHFV antigen, mouse anti-CCHFV Gc monoclonal 11E7 (BEI Resources) was applied at 500 ng per ml in permwash and incubated at room temperature for 2 h. Plates were washed with permwash and bound antibody detected with horseradish peroxidase-conjugated donkey anti-mouse IgG (Jackson Immuno Research) applied at 1:2,000 in permwash. Plates were incubated at room temperature for 2 h and then washed with permwash. Plates were developed with TrueBlue peroxidase substrate (Seracare) and foci counted with an S6 Universal analyser and Immunospot software (Cellular Technology Limited). To calculate per cent infectivity, the challenge virus was incubated in L-15 media supplemented with 2% heat-inactivated fetal bovine serum, penicillin and streptomycin alone in parallel to serum-treated samples and data reported as (number of foci in serum-treated samples/number of foci in input) X 100. Non-linear regression was performed using GraphPad Prism 7.03 software.

Serum cytokine levels.

Serum samples were inactivated using y-irradiation (10 Mrad) and removed from the maximum containment laboratory. Serum samples were then diluted 1:2 in serum matrix for analyses by using the Milliplex Non-Human Primate Magnetic Bead Panel (Millipore) according to the manufacturer's instructions. Concentrations of cytokines were determined for all samples by using the Bio-Plex 200 System (BioRad Laboratories).

Statistical analysis.

Data were analysed with one-way analysis of variance and a Tukey's multiple comparison test comparing infection routes on examination days. Data were not analysed past 7 dpi as overall group numbers were greatly reduced. This study was not specifically designed for

statistical evaluation as group numbers were small, and any animal loss therefore negatively impacts statistical testing.

Supplementary Material

Refer to Web version on PubMed Central for supplementary material.

Acknowledgements

We thank the staff of the Rocky Mountain Veterinary Branch, Division of Intramural Research (DIR), National Institute of Allergy and Infectious Diseases (NIAID), National Institutes of Health (NIH) for assistance with animal care and clinical and pathological veterinary services, and Atsushi Okumura for veterinary expertise throughout the study. We would also like to thank the members of the Visual and Medical Arts (DIR, NIAID, NIH) for aid in figure development. This work was funded by the Intramural Research Programme of the NIAID, NIH.

References

1. Bente DA et al. Crimean-Congo hemorrhagic fever: history, epidemiology, pathogenesis, clinical syndrome and genetic diversity. Antiviral Res. 100, 159–189 (2013). [PubMed: 23906741]
2. Hoogstraal H The epidemiology of tick-borne Crimean-Congo hemorrhagic fever in Asia, Europe, and Africa. J. Med. Entomol. 15, 307–417 (1979). [PubMed: 113533]
3. Spengler JR et al. A chronological review of experimental infection studies of the role of wild animals and livestock in the maintenance and transmission of Crimean-Congo hemorrhagic fever virus. Antiviral Res. 135, 31–47 (2016). [PubMed: 27713073]
4. Bente DA et al. Pathogenesis and immune response of Crimean-Congo hemorrhagic fever virus in a STAT-1 knockout mouse model. J. Virol. 84, 11089–11100 (2010). [PubMed: 20739514]
5. Bereczky S et al. Crimean-Congo hemorrhagic fever virus infection is lethal for adult type I interferon receptor-knockout mice. J. Gen. Virol. 91, 1473–1477 (2010). [PubMed: 20164263]
6. Zivcec M et al. Lethal Crimean-Congo hemorrhagic fever virus infection in interferon α/β receptor knockout mice is associated with high viral loads, proinflammatory responses, and coagulopathy. J. Infect. Dis 207, 1909–1921 (2013). [PubMed: 23417661]
7. Cevik MA et al. Viral load as a predictor of outcome in Crimean-Congo hemorrhagic fever. Clin. Infect. Dis. 45, e96–e100 (2007). [PubMed: 17806044]
8. Onguru P et al. Coagulopathy parameters in patients with Crimean-Congo hemorrhagic fever and its relation with mortality. J. Clin. Lab. Anal. 24, 163–166 (2010). [PubMed: 20486197]
9. Duh D et al. Viral load as predictor of Crimean-Congo hemorrhagic fever outcome. Emerg. Infect. Dis. 13, 1769–1772 (2007). [PubMed: 18217568]
10. Whitehouse CA Crimean-Congo hemorrhagic fever. Antiviral Res. 64, 145–160 (2004). [PubMed: 15550268]
11. Ergonul O Crimean-Congo haemorrhagic fever. Lancet Infect. Dis. 6, 203–214 (2006). [PubMed: 16554245]
12. Kubar A et al. Prompt administration of Crimean-Congo hemorrhagic fever (CCHF) virus hyperimmunoglobulin in patients diagnosed with CCHF and viral load monitorization by reverse transcriptase-PCR. Jpn J. Infect. Dis. 64, 439–443 (2011). [PubMed: 21937830]
13. Swanepoel R et al. The clinical pathology of Crimean-Congo hemorrhagic fever. Rev. Infect. Dis 11(Suppl.4), S794–S800 (1989). [PubMed: 2749111]
14. Vorou R, Pierroutsakos IN & Maltezou HC Crimean-Congo hemorrhagic fever. Curr. Opin. Infect. Dis. 20, 495–500 (2007). [PubMed: 17762783]
15. Soares-Weiser K, Thomas S, Thomson G & Garner P Ribavirin for Crimean-Congo hemorrhagic fever: systematic review and meta-analysis. BMC Infect. Dis. 10, 207 (2010). [PubMed: 20626907]
16. Keshtkar-Jahromi M et al. Crimean-Congo hemorrhagic fever: current and future prospects of vaccines and therapies. Antiviral Res. 90,85–92 (2011). [PubMed: 21362441]

17. Fagbami AH, Tomori O, Fabiyi A & Isoun TT Experimantal Congo virus (Ib -AN 7620) infection in primates. Virologie 26, 33–37 (1975). [PubMed: 814708]
18. Smirnova SE A comparative study of the Crimean hemorrhagic fever-Congo group of viruses. Arch. Virol. 62, 137–143 (1979). [PubMed: 94536]
19. Fajs L et al. Molecular epidemiology of Crimean-Congo hemorrhagic fever virus in Kosovo. PLoS Negl. Trop. Dis. 8, e2647 (2014).
20. Brining DL et al. Thoracic radiography as a refinement methodology for the study of H1N1 influenza in cynomologus macaques (Macaca fascicularis). Comp. Med. 60, 389–395 (2010). [PubMed: 21262125]
21. Causey OR, Kemp GE, Madbouly MH & David-West TS Congo virus from domestic livestock, African hedgehog, and arthropods in Nigeria. Am. J. Trop. Med. Hyg. 19, 846–850 (1970). [PubMed: 5453910]
22. Duh D et al. The complete genome sequence of a Crimean-Congo hemorrhagic fever virus isolated from an endemic region in Kosovo. Virol. J. 5, 7 (2008). [PubMed: 18197964]
23. Safronetz D et al. Pathophysiology of hantavirus pulmonary syndrome in rhesus macaques. Proc. Natl Acad. Sci. USA 111, 7114–7119 (2014). [PubMed: 24778254]
24. Burt FJ et al. Immunohistochemical and in situ localization of Crimean-Congo hemorrhagic fever (CCHF) virus in human tissues and implications for CCHF pathogenesis. Arch. Pathol. Lab. Med. 121, 839–846 (1997). [PubMed: 9278612]
25. Ergonul O et al. Cytokine response in Crimean-Congo hemorrhagic fever virus infection. J. Med. Virol. 89, 1707–1713 (2017). [PubMed: 28547808]
26. Kaya S et al. Sequential determination of serum viral titers, virus-specific IgG antibodies, and TNF-α, IL-6, IL-10, and IFN-y levels in patients with Crimean-Congo hemorrhagic fever. BMC Infect. Dis. 14, 416 (2014). [PubMed: 25066751]
27. Papa A et al. Cytokines as biomarkers of Crimean-Congo hemorrhagic fever. J. Med. Virol. 88, 21–27 (2016). [PubMed: 26118413]
28. Saksida A, Wraber B & Avsic-Zupanc T Serum levels of inflammatory and regulatory cytokines in patients with hemorrhagic fever with renal syndrome. BMC Infect. Dis. 11, 142 (2011). [PubMed: 21605369]
29. Ergonul O, Tuncbilek S, Baykam N, Celikbas A & Dokuzoguz B Evaluation of serum levels of interleukin (IL)-6, IL-10, and tumor necrosis factor-a in patients with Crimean-Congo hemorrhagic fever. J. Infect. Dis. 193, 941–944 (2006). [PubMed: 16518755]
30. Wang F et al. RNAscope: a novel in situ RNA analysis platform for formalin-fixed, paraffin-embedded tissues. J. Mol. Diagn. 14, 22–29 (2012). [PubMed: 22166544]

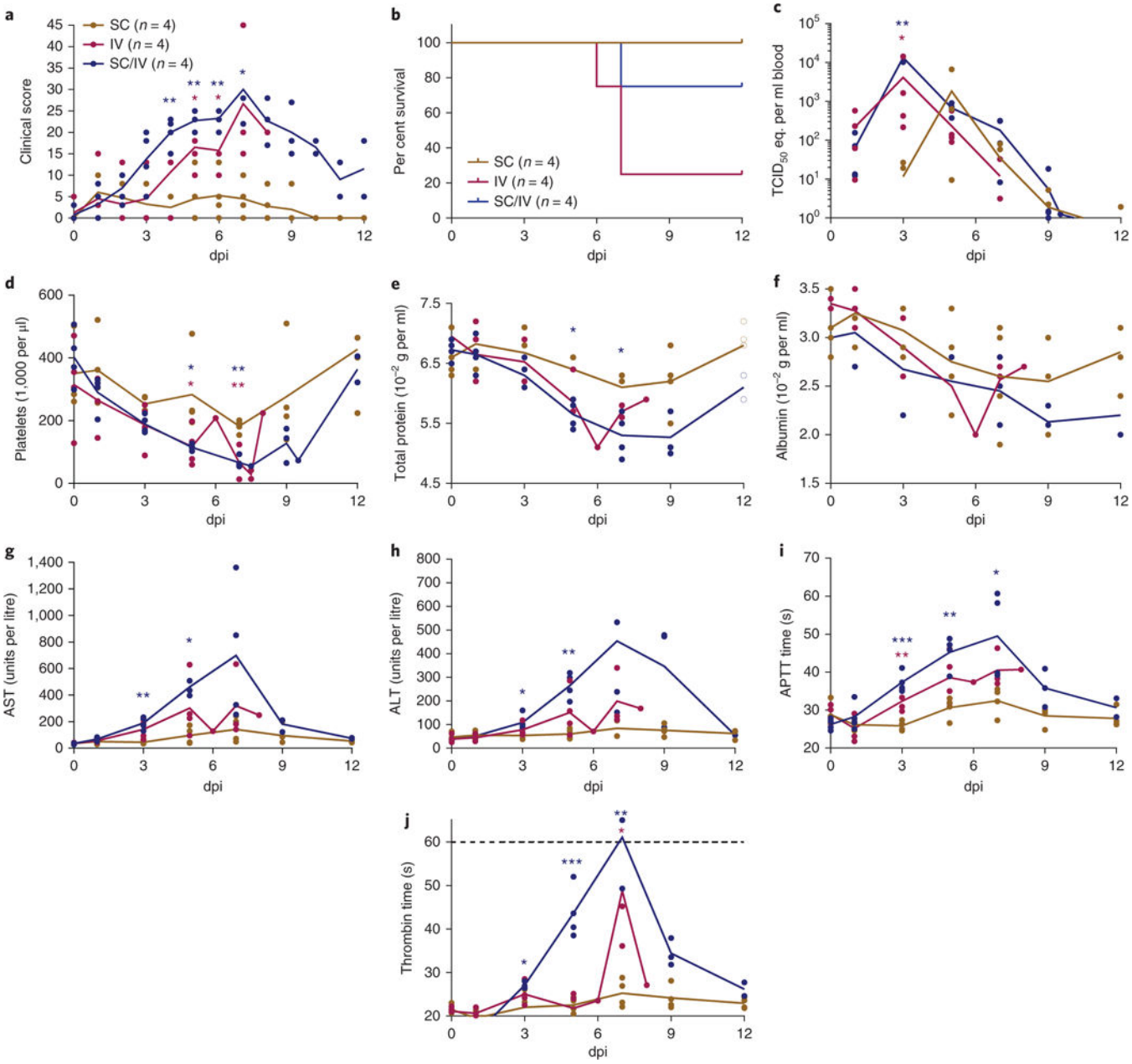

Fig. 1 |. Clinical parameters for CCHFV-infected cynomolgus macaques.

Parameters were measured for each animal on days of examination and at time of euthanasia (n = 4 animals per inoculation route). Graphs represent a single biological experiment. **a,** Clinical score, with euthanasia mandated at a score of 35. **b**, Survival curves. **c**, Viral RNA load in whole blood of animals, by infection route, standardized to $TCID_{50}$ equivalents of the stock challenge virus RNA per ml of whole blood. **d**, Platelet counts. **e**, Total protein levels. **f**, Albumin levels. **g**, Aspartate aminotransferase (AST) levels. **h**, Alanine aminotransferase (ALT) levels. **i**, Activated partial thromboplastin time (APTT). **j**, Thrombin time; a 60-second clotting time is the preset limit to this test, as surpassed by 4 of 12 animals. Data are shown as individual points with lines representing the mean response by

inoculation route, except in the case of panel **b**, which depicts survival based on inoculation route. Statistical analysis by one-way analysis of variance and a Tukey's multiple comparison test defines significance between inoculation routes on given examination days. All statistically significant differences represent a difference between either the intravenous- or SC/IV-inoculated group (as designated by colour) and the subcutaneous-inoculated group. Analysis was performed only through to 7 dpi due to reduced group numbers after this point. *P<0.05, **P< 0.005, ***P<0.001. Individual P values are as follows (95% confidence interval): **a**, SC/IV 4 dpi = 0.0019, intravenous 5 dpi = 0.0174, SC/IV 5 dpi = 0.0013, intravenous 6 dpi = 0.0273, SC/IV 6 dpi = 0.0011, SC/IV 7 dpi = 0.0310; **c**, intravenous 3 dpi = 0.0265, SC/IV 3 dpi = 0.0032; **d**, intravenous 5 dpi = 0.0491, SC/IV 4 dpi = 0.0459, intravenous 7 dpi = 0.0040, SC/IV 7 dpi = 0.0025; **e**, SC/IV 5 dpi = 0.0404, SC/IV 7 dpi = 0.0155; **g**,SC/IV3dpi = 0.0072, SC/IV 5 dpi = 0.0130; **h**, SC/IV 3 dpi = 0.0487, SC/IV 5 dpi = 0.0047; **i**,intravenous3dpi = 0.0073, SC/IV 3 dpi = 0.001, SC/IV 5 dpi = 0.0050, SC/IV 7 dpi = 0.0368; **j**, SC/IV 3 dpi = 0.0401, SC/IV5dpi = 0.0001,intravenous7dpi = 0.0222, SC/IV 7 dpi = 0.0013. IV, intravenous; SC, subcutaneous.

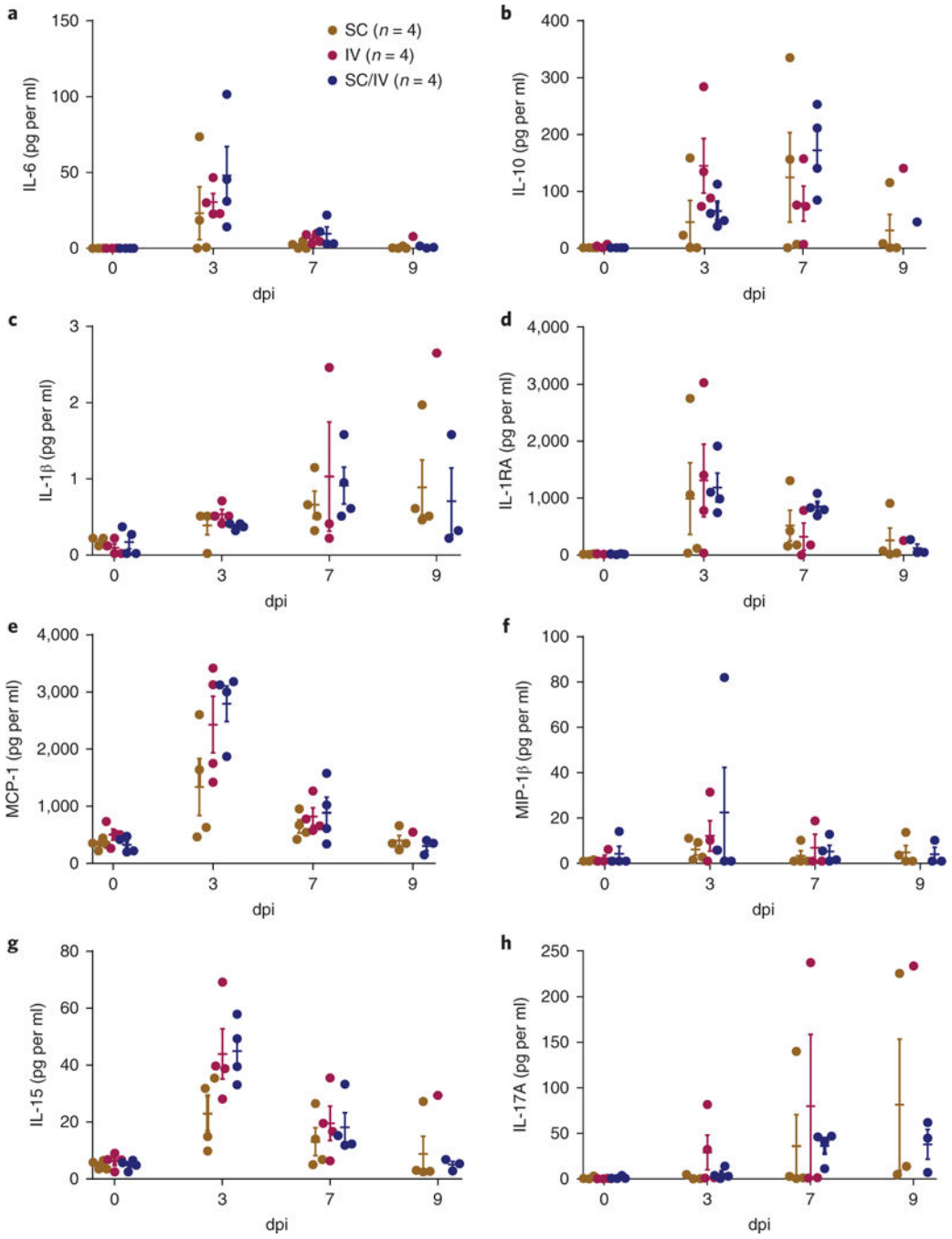

Fig. 2 |. Profile of immune factors by infection route in CCHFV-infected cynomolgus macaques. Concentrations of cytokine or chemokine levels were determined in serum samples collected during clinical exams using a multiplex NHP cytokine detection kit. **a**, IL-6. **b**, IL-10. **c**, IL-1β. **d**, IL-1RA. **e**, MCP-1. **f,** MIP-1β. **g**, IL-15. **h**, IL-17A. Examination days depicted represent the onset of symptoms (3 dpi), terminal disease (7dpi) or onset of convalescence (9 dpi). Results are of a single biological experiment with $n = 4$ animals per inoculation route. Data points are graphed individually with standard error of the mean for each inoculation route. Statistical analysis by one-way analysis of variance and a Tukey's multiple

comparison test showed no significance between inoculation routes on given examination days.

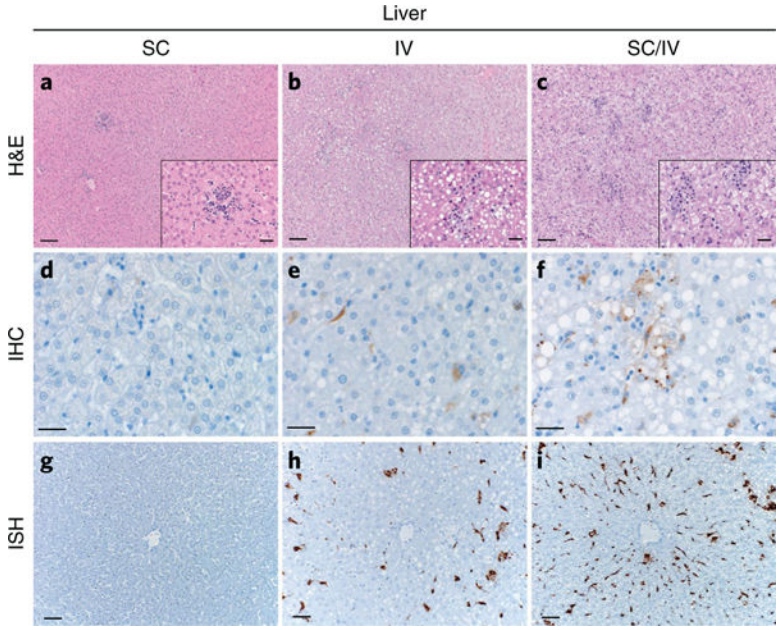

Fig. 3 |. Histopathology, immunohistochemistry and in situ hybridization (viral genomic RNA) of the liver from CCHFV-infected cynomolgus macaques.

a-c, Haematoxylin and eosin (H&E) ×100, inset ×400. The panels show multifocal, minimal lymphohistiocytic infiltrates (**a**); multifocal, minimal lymphohistiocytic infiltrates (**b**); and multifocal mild-moderate lymphohistiocytic infiltrates (**c**). Scale bars,50 μm (main),20 μm (inset). **d-f**, Immunohistochemistry (IHC) ×400. The panels show no immunoreactivity (**d**); rare immunoreactivity in hepatocytes, Kupffer cells and endothelial cells (**e**); and scattered to moderate immunoreactivity in hepatocytes, Kupffer cells and endothelial cells (**f**). Scale bars, 20 μm. **g-i**, In situ hybridization (ISH) depicting viral RNA x100. The panels show no immunoreactivity (**g**); moderate immunoreactivity in hepatocytes, Kupffer cells and endothelial cells (**h**); and moderate-numerous immunoreactivity in hepatocytes, Kupffer cells and endothelial cells (**i**). Scale bars,50 μm. Figures are representative of all animals within the inoculation group (n = 4 animals).

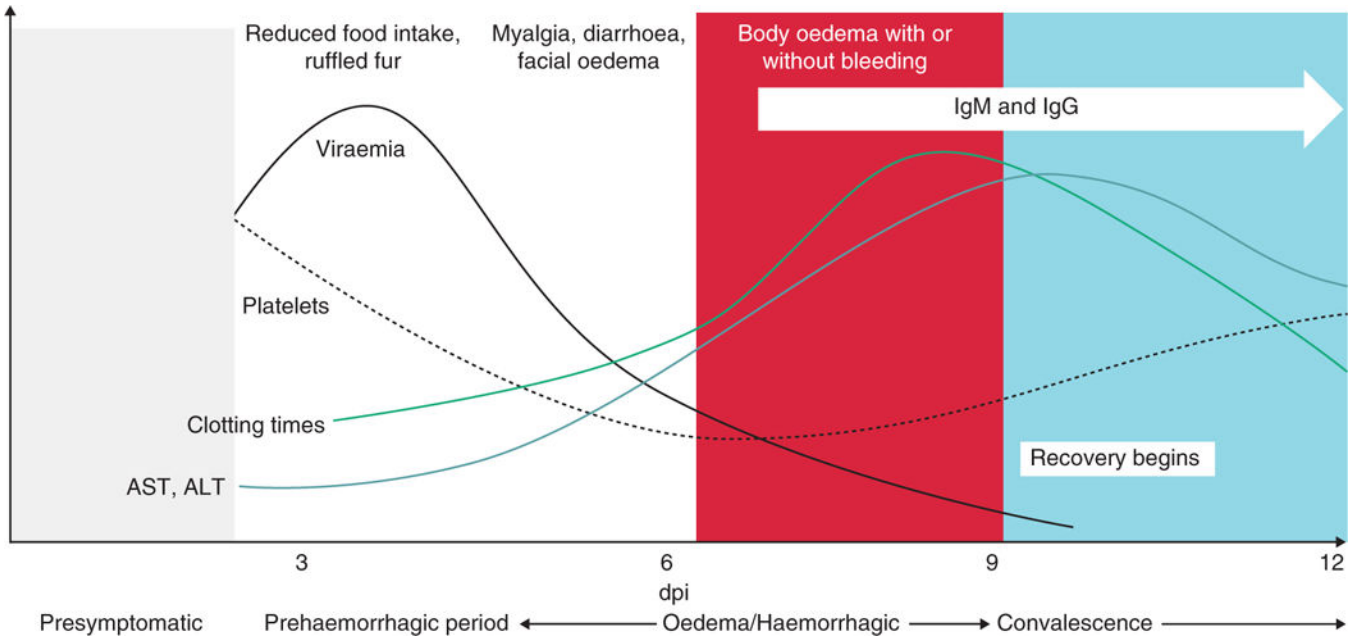

Fig. 4 |. Profile of CCHF disease in cynomolgus macaques.

As with human disease, the macaque disease progression may be divided into four periods, with viraemia escalating as platelets drop in the presymptomatic and prehaemorrhagic period, followed by a rise in liver enzymes and elongation in clotting times in the haemorrhagic period. These clinical signs gradually return to normal as the animals enter convalescence.